General Disclaimer

One or more of the Following Statements may affect this Document

- This document has been reproduced from the best copy furnished by the organizational source. It is being released in the interest of making available as much information as possible.

- This document may contain data, which exceeds the sheet parameters. It was furnished in this condition by the organizational source and is the best copy available.

- This document may contain tone-on-tone or color graphs, charts and/or pictures, which have been reproduced in black and white.

- This document is paginated as submitted by the original source.

- Portions of this document are not fully legible due to the historical nature of some of the material. However, it is the best reproduction available from the original submission.

NASA TECHNICAL MEMORANDUM

NASA TM X-71766

NASA TM X-71766

FLOW VISUALIZATION OF DISCRETE HOLE FILM COOLING FOR GAS TURBINE APPLICATIONS

by Raymond S. Colladay and Louis M. Russell
Lewis Research Center
Cleveland, Ohio 44135

TECHNICAL PAPER to be presented at
Gas Turbine Heat Transfer Session of the
Winter Annual Conference of the
American Society of Mechanical Engineers
Houston, Texas, November 30 - December 4, 1975

FLOW VISUALIZATION OF DISCRETE HOLE FILM COOLING FOR GAS TURBINE APPLICATIONS

Raymond S. Colladay and Louis M. Russell

Lewis Research Center

E-8418

ABSTRACT

Film injection from discrete holes in a three row staggered array with 5-diameter spacing is studied for three different hole angles: (1) normal, (2) slanted 30° to the surface in the direction of the mainstream, and (3) slanted 30° to the surface and 45° laterally to the mainstream. The boundary layer thickness-to-hole diameter ratio and Reynolds number are typical of gas turbine film cooling applications. Two different injection locations are studied to evaluate the effect of boundary layer thickness on film penetration and mixing. Detailed streaklines showing the turbulent motion of the injected air are obtained by photographing very small neutrally buoyant helium filled "soap" bubbles which follow the flow field. Unlike smoke, which diffuses rapidly in the high turbulent mixing region associated with discrete hole blowing, the bubble streaklines passing downstream injection locations are clearly identifiable and can be traced back to their origin. Visualization of surface temperature patterns obtained from infrared photographs of a similar film cooled surface are also included.

NOMENCLATURE

D = film injection hole diameter

m = film-to-mainstream mass velocity ratio or blowing rate (u_f/u_∞ for constant density)

u_f = film injection velocity

u_∞ = freestream velocity

u^+ = dimensionless velocity, $u_\infty/\sqrt{\tau_w/\rho}$

y = coordinate normal to the surface

y^+ = dimensionless distance, $y\sqrt{\tau_w/\rho}/\nu$

δ = boundary layer thickness

θ = boundary layer momentum thickness

ν = kinematic viscosity

ρ = density

τ_w = wall shear stress

INTRODUCTION

Increases in turbine inlet temperature and pressure have reached the point where heat flux levels are too high to adequately cool hot section gas turbine components by convection alone. Some film cooling is generally required to protect the metal parts from the hot gas stream. The most practical method currently used for film cooling aircraft turbines is to inject the cooling air from discrete holes in the surface of the blade. It is important that the film be injected in the most efficient manner possible in order to provide the desired heat transfer protection with a minimum disruption of the mainstream. Poorly designed film injection schemes can lead to mainstream momentum losses which severly reduce turbine aerodynamic efficiency and, in some instances, even increase heat transfer to the surface.

There has been considerable emphasis recently in experimental heat transfer studies related to discrete hole film cooling. The University of Minnesota investigated adiabatic wall film effectiveness and augmented heat transfer coefficients due to blowing for one hole and a single row of holes at various injection angles and center-to-center spacings. Reference 1 is the last in a series of reports on this study. It includes a complete bibliography of earlier reports. A similar study for a single row of injection holes with a freestream static pressure distribution typical of turbine blade applications is reported in Ref. 2.

Stanford University is investigating the heat transfer characteristics of full coverage film cooling from a staggered array of discrete holes spaced either 5 or 10 diameters apart. Some preliminary results from this study are given in Ref. 3. Reference 4 is a data report containing all of the test results for both normal and 30 degree injection. An experimental investigation of the adiabatic wall film effectiveness associated with full coverage film cooling from compound angle injection at various hole spacings has been reported in Ref. 5. Analytical and experimental work in this area has been the subject of several reports from Imperial College, (6 and 7)

While all of these investigations have contributed to the quantitative data needed to develop reliable analytical models of film cooling, they have also suggested the need for a better understanding of the complex fluid dynamics encountered when film air is injected through discrete holes into a turbulent boundary layer. Such insight can only be provided through good flow visualization studies. Visualization of the flow field associated with discrete hole film cooling is helpful to fully understand and appreciate the complex interaction of the film and the mainstream. Some effort was made, as reported in Ref.

1, to visualize the flow field surrounding a single injection hole using CO_2 fog. However, the fog diffused so rapidly due to the high turbulent mixing in the injection region that only the large scale turbulent motion near the hole was visible.

In the present study, air seeded with small neutrally buoyant helium-filled bubbles, was injected into a turbulent boundary layer through discrete holes in the test surface of an ambient air wind tunnel. The paths traced by the bubbles map streakline patterns of the injected film air mixing with the mainstream. Unlike smoke or fog which diffuses rapidly, the bubble streaklines are clearly identifiable as continuous thread-like streaks which can be traced through the film injection region.

Streakline patterns of the flow field associated with film injection from discrete holes in a three row staggered array with 5-diameter spacing are presented for three different hole angles typically encountered in turbine cooling applications. The holes were angled (1) normal to the surface, (2) slanted 30° to the surface in the direction of the mainstream, and (3) slanted 30° to the surface and 45° laterally to the mainstream. The momentum thickness Reynolds number just upstream of the injection holes was 2165 and the boundary layer thickness-to-hole diameter was 1.75. A boundary layer thickness-to-hole diameter of 2.4 at the same Reynolds number was also run by moving the injection location further downstream from the inlet nozzle. Infrared photographs of a similar film cooled wall were taken to show the surface temperature pattern resulting from discrete hole film cooling.

EXPERIMENTAL APPARATUS

Bubble Generator

The system for generating neutrally-buoyant bubbles, described in detail in the manufacturer's report[8], consists of a head, which is the device that actually forms the bubbles, and a console containing micrometering valves which control the flow of helium, bubble solution, and air to the head. A drawing illustrating the basic features of the head is shown in Fig. 1. Neutrally buoyant helium- filled bubbles about 1 mm in diameter, form on the tip of the concentric tubes and are blown off the tip by a continuous blast of air flowing through the shroud passage. Bubble solution flows through the annular passage and is formed into a bubble inflated with the helium passing through the inner concentric tube. The desired bubble size and neutral buoyancy are achieved by proper adjustment of air, bubble solution, and helium flow rates. As many as 300 bubbles per second can be formed in this device.

Rig

The flow visualization test rig, shown in schematic form in Fig. 2 consists of a transparent plastic tunnel through which room air is drawn into an altitude exhaust line. It is a simple construction providing flexibility for testing a large number of film injection hole geometries and boundary layer configurations appropriate to turbine and combustor cooling applications. The test configuration for this report consisted of a zero pressure gradient mainstream flow over a flat surface containing discrete film injection holes. At the point of injection, the mainstream boundary layer was fully turbulent. A further description of the details of the rig are given in Ref. 9. There are three separate air flow sources: (1) the primary mainstream air; (2) the bubble generator air; and (3) the secondary film injection air.

The tunnel, 0.381 by 0.152 meters in cross-section, is sectioned into four parts; a test section 0.61 m long and three spacing sections each 0.91 m long. The sections can be put in any order to allow for a boundary layer development length upstream of the first film injection location anywhere from several centimeters to over 2.7 meters. Having the option of injecting the film air at different axial locations downstream of the inlet provides the flexibility of independent control of the following three related variables: injection-to-mainstream velocity ratio u_c/u_∞, the boundary layer thickness-to-injection hole diameter δ/D, and the momentum thickness Reynolds number at the point of injection. A long boundary layer development length is needed to cover the high range of the δ/D ratio because the minimum hole diameter is limited to about 1.27 cm to avoid excessive bubble breakage in the holes.

The helium filled bubbles are injected into a plenum which serves as a collection chamber for the bubbles and the film air. The air, seeded with the bubbles, then passes through the film injection holes in the floor of the test section. The small quantity of air used by the bubble generator to blow the bubbles off the tip of the annulus as they form, ends up as part of the film air in the plenum. However, this bubble air flow cannot be varied since it is adjusted and then fixed to give optimum bubble formation. Consequently, to provide variable film injection air flow rates, additional secondary air is also supplied to the plenum. The plenum box is clamped onto the bottom of the test section for easy removal when another test plate with a different hole configuration is to be tested. Rotometers were used to measure the helium and bubble generator air flow rates and a hot wire flow meter was used in the secondary air leg for accurate measurement over a wide range of film air flow rates.

When the bubbles pass through the film injection holes, they are illuminated by a high intensity quartz arc lamp. The resulting reflection off the bubble surface appears as a streak across the photographic film if the exposure is relatively slow. Sometimes two reflections appear on the same bubble giving a double streak. The light beam was directed axially down the tunnel as shown in the sketch in Fig. 2. With a well-focused and collimated light beam, the bubbles are illuminated as soon as they leave the holes without the beam striking any of the tunnel surfaces. This insures good contrast with a bright bubble streak against a black background.

Test Section

The 0.38 by 0.61 m floor of the test section which contains the film injection holes is easily removed to allow bottom plates with different hole configurations to be installed without affecting the rest of the test section or the plenum chamber. The floor and back side of the test section are made of wood and finished glossy black to give maximum contrast with the bubble streaklines. The top and front face are clear plastic.

Three different film injection arrays were studied. Sketches of the three configurations are given in Fig. 3. They are (1) normal injection with the holes oriented normal to the surface, (2) slanted in-line injection with the holes angled 30° to the

1, to visualize the flow field surrounding a single injection hole using CO_2 fog. However, the fog diffused so rapidly due to the high turbulent mixing in the injection region that only the large scale turbulent motion near the hole was visible.

In the present study, air seeded with small neutrally buoyant helium-filled bubbles, was injected into a turbulent boundary layer through discrete holes in the test surface of an ambient air wind tunnel. The paths traced by the bubbles map streakline patterns of the injected film air mixing with the mainstream. Unlike smoke or fog which diffuses rapidly, the bubble streaklines are clearly identifiable as continuous thread-like streaks which can be traced through the film injection region.

Streakline patterns of the flow field associated with film injection from discrete holes in a three row staggered array with 5-diameter spacing are presented for three different hole angles typically encountered in turbine cooling applications. The holes were angled (1) normal to the surface, (2) slanted 30° to the surface in the direction of the mainstream, and (3) slanted 30° to the surface and 45° laterally to the mainstream. The momentum thickness Reynolds number just upstream of the injection holes was 2165 and the boundary layer thickness-to-hole diameter was 1.75. A boundary layer thickness-to-hole diameter of 2.4 at the same Reynolds number was also run by moving the injection location further downstream from the inlet nozzle. Infrared photographs of a similar film cooled wall were taken to show the surface temperature pattern resulting from discrete hole film cooling.

EXPERIMENTAL APPARATUS

Bubble Generator

The system for generating neutrally-buoyant bubbles, described in detail in the manufacturer's report[8], consists of a head, which is the device that actually forms the bubbles, and a console containing micrometering valves which control the flow of helium, bubble solution, and air to the head. A drawing illustrating the basic features of the head is shown in Fig. 1. Neutrally buoyant helium- filled bubbles about 1 mm in diameter, form on the tip of the concentric tubes and are blown off the tip by a continuous blast of air flowing through the shroud passage. Bubble solution flows through the annular passage and is formed into a bubble inflated with the helium passing through the inner concentric tube. The desired bubble size and neutral buoyancy are achieved by proper adjustment of air, bubble solution, and helium flow rates. As many as 300 bubbles per second can be formed in this device.

Rig

The flow visualization test rig, shown in schematic form in Fig. 2 consists of a transparent plastic tunnel through which room air is drawn into an altitude exhaust line. It is a simple construction providing flexibility for testing a large number of film injection hole geometries and boundary layer configurations appropriate to turbine and combustor cooling applications. The test configuration for this report consisted of a zero pressure gradient mainstream flow over a flat surface containing discrete film injection holes. At the point of injection, the mainstream boundary layer was fully turbulent. A further description of the details of the rig are given in Ref. 9. There are three separate air flow sources: (1) the primary mainstream air; (2) the bubble generator air; and (3) the secondary film injection air.

The tunnel, 0.381 by 0.152 meters in cross-section, is sectioned into four parts: a test section 0.61 m long and three spacing sections each 0.91 m long. The sections can be put in any order to allow for a boundary layer development length upstream of the first film injection location anywhere from several centimeters to over 2.7 meters. Having the option of injecting the film air at different axial locations downstream of the inlet provides the flexibility of independent control of the following three related variables: injection-to-mainstream velocity ratio u_c/u_∞, the boundary layer thickness-to-injection hole diameter δ/D, and the momentum thickness Reynolds number at the point of injection. A long boundary layer development length is needed to cover the high range of the δ/D ratio because the minimum hole diameter is limited to about 1.27 cm to avoid excessive bubble breakage in the holes.

The helium filled bubbles are injected into a plenum which serves as a collection chamber for the bubbles and the film air. The air, seeded with the bubbles, then passes through the film injection holes in the floor of the test section. The small quantity of air used by the bubble generator to blow the bubbles off the tip of the annulus as they form, ends up as part of the film air in the plenum. However, this bubble air flow cannot be varied since it is adjusted and then fixed to give optimum bubble formation. Consequently, to provide variable film injection air flow rates, additional secondary air is also supplied to the plenum. The plenum box is clamped onto the bottom of the test section for easy removal when another test plate with a different hole configuration is to be tested. Rotometers were used to measure the helium and bubble generator air flow rates and a hot wire flow meter was used in the secondary air leg for accurate measurement over a wide range of film air flow rates.

When the bubbles pass through the film injection holes, they are illuminated by a high intensity quartz arc lamp. The resulting reflection off the bubble surface appears as a streak across the photographic film if the exposure is relatively slow. Sometimes two reflections appear on the same bubble giving a double streak. The light beam was directed axially down the tunnel as shown in the sketch in Fig. 2. With a well-focused and collimated light beam, the bubbles are illuminated as soon as they leave the holes without the beam striking any of the tunnel surfaces. This insures good contrast with a bright bubble streak against a black background.

Test Section

The 0.38 by 0.61 m floor of the test section which contains the film injection holes is easily removed to allow bottom plates with different hole configurations to be installed without affecting the rest of the test section or the plenum chamber. The floor and back side of the test section are made of wood and finished glossy black to give maximum contrast with the bubble streaklines. The top and front face are clear plastic.

Three different film injection arrays were studied. Sketches of the three configurations are given in Fig. 3. They are (1) normal injection with the holes oriented normal to the surface, (2) slanted in-line injection with the holes angled 30° to the

surface and in-line with the mainstream, and (3) compound angle injection with the holes again 30° to the surface, but rotated 45° laterally to the mainstream. In all three cases, the holes were spaced 5 diameters apart as measured from the hole centerline. The holes formed a staggered array representing the center portion of three rows of holes. In Fig. 3(b) and (c), the hole axes for both the in-line and compound angle holes make an angle of 30° with the plane of the paper. Tubes which extend into the plenum were inserted into the holes in the plate and finished off flush with the test surface to provide a hole length to diameter ratio typical of aircraft turbine applications. The delivery tubes for this study had a 1.27 cm inner diameter and were 5.1 cm long.

RESULTS AND DISCUSSION

A fully turbulent boundary layer existed in the region of the film injection holes and the freestream turbulence was negligibly small for all of the results presented in this paper. The film-to-mainstream velocity ratio was varied by changing the mass flow rate of the secondary or film air while keeping the mainstream velocity constant at 15.5 m/sec. The velocity profile through the boundary layer was surveyed just upstream of the injection holes. The dimensionless profile at the duct centerline in Fig. 4 shows the typical logarithmic distribution in the wall region, characteristic of a turbulent boundary layer on a smooth wall. Surveys off the centerline showed less than a 1 percent spanwise variation in the profile within the injection region. The boundary layer thickness, defined by the 99 percent value of the freestream velocity, was 2.22 cm. The boundary layer thickness-to-injection hole diameter ratio was then 1.75 at the upstream injection location. The boundary layer momentum thickness and shape factor were 0.215 cm and 1.31, respectively, and the momentum thickness Reynolds number was 2165 at the upstream hole location.

Photographs of the film streaklines were taken both from the top looking down on the test surface and from the side looking through the boundary layer. The two viewing angles are illustrated in Fig. 5 which shows the test section with two cameras mounted in the positions used when taking photographs. The top view photographs show the spreading characteristics of the film as it leaves the holes and the side view photographs show the degree of penetration of the film into the mainstream relative the boundary layer thickness and the surface. All of the side view photographs were taken with the two outer holes in the four hole array plugged to give a plane view of the two center holes. The film from the upstream hole passes directly over the downstream hole.

Normal Injection. Streaklines traced by a film injected into a turbulent boundary layer from an array of holes oriented normal to the surface are shown in Fig. 6. The streaklines in the figures are black on a white background because the photographs in this paper are negative images printed from color transparencies. Top and side view photographs are included for a low ($m = 0.3$) and a high ($m = 0.8$) blowing rate. Also included is a close-up view of the region surrounding the upstream hole. The top view clearly illustrates the counter-rotating vortices extending downstream of each injection hole. This vortex pattern has been well documented in earlier studies. The top view also shows that the film spreads about one and a half hole diameters for a blowing rate of $m = 0.3$ and slightly more at the high blowing rate.

From the side view, it is noted that the film separates from the surface and penetrates into the freestream even at a low blowing rate of $m = 0.3$. The boundary layer thickness δ just upstream of the first injection hole is indicated on the side view photograph. At the high blowing rate, most of the film mixes with the freestream rather than providing a protective film adjacent to the surface.

Notice the sharp "kinks" in the streaklines in the close-up view, particularly at the high blowing rate. The tortuous path traced by a bubble indicates a very high intensity, small scale turbulence structure in the vortex region just downstream of an injection hole. This high turbulence is detrimental because it increases the heat transfer coefficient and causes rapid mixing of the film air with the mainstream. As the bubbles get caught up in one of the vortices, their trajectory is in a direction nearly normal to the surface, suggesting a very high velocity transfer of mass between the wall region and the outer boundary layer. There is also evidence of recirculating flow since some of the streaklines slope back upstream.

Slanted In-line Injection. The streakline pattern associated with film injection from holes angled 30° to the surface, in-line with the mainstream is given in Fig. 7. For this geometry, blowing rates having nominal values of $m = 0.3$, 0.8, and 1.4, were photographed. A top and side full field view, and a close-up side view of the region surrounding the downstream hole are included. Notice that in general, the streaklines are much smoother than with normal injection, indicating a much larger scale and lower intensity turbulence for 30° injection. Only at the highest blowing rate do the streaklines exhibit the character indicative of high intensity, small scale turbulence. The counter-rotating vortex pattern is not nearly as evident as it was for the normal injection case. Evidence of entrainment of the freestream fluid down to the wall can be seen however, as the streaklines coming from the center of the hole wrap around the outside of the jet. The pattern is more subtle than with normal holes because the scale at which the streaklines interwind is much larger--on the order of the hole diameter. As can be seen from the top view, there is almost no spreading of the film as it extends downstream even when passing over another injection hole. Most of the upstream film tends to split to either side of the downstream jet.

At a blowing rate of about $m = 0.5$, the film begins to separate from the surface. At $m = 0.8$, the full field, side view photograph clearly shows that the film has separated from the surface allowing the mainstream air to wrap around beneath the jets. At the high blowing rate ($m = 1.4$), the film penetrates into the freestream and offers little protection to the surface. Also, as one would expect, the downstream film has a steeper trajectory across the boundary layer because of the momentum deficit in the incident boundary layer near the wall created by the upstream injection.

The close-up view shows the downstream jet passing right through the film from the upstream hole. Note also the high turbulence generated for the case of $m = 1.4$ compared to the lower blowing rates. It has been observed that when the velocity of the jet

exceeds that of the mainstream, there is a change in the character of the turbulence near the injection holes. When $m < 1$, the streaks are smooth and gently undulating. When $m > 1$, very jagged streaks appear.

Compound Angle Injection. The distinctive features of the streakline pattern associated with film injection at a compound angle 30° to the surface and 45° lateral to the mainstream are illustrated in Figs. 8 and 9. For this injection configuration, the oblique angle that the film makes with the mainstream generates a single, strong vortex filament downstream of each hole. This vortex motion begins forming at blowing rates of about $m = 0.3$[8(a)] and becomes most pronounced at blowing rates between $m = 0.7$ and $m = 0.9$. Notice the very tight "winding" of the streaklines in Fig. 8(b) for a blowing rate of $m = 0.75$. A close-up top view of the region surrounding the upstream injection location for this blowing rate is shown in Fig. 8(c). The most important feature of compound angle injection is that this strong vortex motion keeps the film attached to the surface even at the high blowing rates. This can be seen from Fig. 9 which compares the compound angle injection at a low and a high blowing rate. Notice that there is very little difference in the penetration distance between a blowing rate of 0.3 and 0.9. Even at a velocity ratio of 0.9, the film remains attached to the surface. Note particularly how the downstream film lies underneath the film from the upstream hole. Recall in Fig. 7(b) that for the in-line injection, most of the film separated from the surface at a blowing rate of $m = 0.8$.

Effect of Boundary Layer Thickness. To determine what effect the initial boundary layer thickness has on the distance that the film jet penetrates into the mainstream, the 30° in-line injection configuration was re-run with a thicker boundary layer by moving the injection location further downstream from the inlet nozzle. A side view photograph showing the streakline pattern is given in Fig. 10. The boundary layer thickness was increased 37 percent over that which existed for the results discussed previously. The blowing rate was 0.8, the same as in Fig. 7(b). The freestream velocity was decreased to give the same Reynolds number at the point of injection as in the earlier results. The upstream film jet penetrates further with the thicker boundary layer, but the penetration relative to the boundary layer thickness appears to be about the same. The trajectory of the downstream jet looks the same in both figures which indicates that its penetration is controlled more by the upstream injection than the initial boundary layer thickness.

Infrared Thermal Image. The previous pictures have shown what happens to a film once it is injected into the boundary layer. Figure 11 shows how the surface temperature responds to the same discrete hole film cooling. Infrared pictures of a film cooled test plate run in a hot gas tunnel were taken with 30° slanted in-line[11(a)] and 30° by 45° compound angle[11(b)] injection holes. The mainstream flow is from left to right in the photographs. In both configurations, the holes were in a single row and spaced 2 diameters apart. These results, obtained in another experimental test rig, depart somewhat from the streakline results presented earlier. They are included here to show that the discrete character of the film is preserved in the temperature distribution of the wall. The test plate was flat with a zero pressure gradient mainstream flow. Film injection holes were 0.125 mm in diameter, and the freestream Mach number was 0.6.

The photographs are actual thermal images of the wall surface. Radiation emitted from the surface was recorded on infrared film which can be computer processed to give quantitative temperature data. The hot regions on the surface appear light because they radiate more energy. Conversely, the dark regions are cool. Dark plumes caused by the cool film are visible extending downstream from each hole. The mass velocity ratio $(\rho u)_f/(\rho u)_\infty$ for these tests was 0.5. Notice that the wall temperature pattern remains discrete even with two diameter spacing and that the low temperature streaks run nearly parallel to the mainstream flow even when the film jet is injected 45° laterally to the mainstream.

CONCLUDING REMARKS

A film injected into a turbulent boundary layer from discrete holes remains discrete as the jets extend downstream. To provide good film coverage on the surface, holes should be spaced not more than 5 diameters apart, and much closer for only one or two rows of holes. If a large number of holes are used in a closely packed array, the design should be tailored with variable lateral and axial spacing to best utilize the cumulative build-up of film.

The film should be injected at as shallow an angle to the freestream as possible within the limits set by fabrication constraints. Normal injection is a very inefficient method of film cooling for turbine cooling applications because the film separates from the surface even at low blowing rates. A counter-rotating vortex motion downstream of the injection hole generates excessive turbulent mixing which dissipates the film, increases the heat transfer coefficient, and increases aerodynamic losses in the turbine.

For injection holes angled 30° to the surface in-line with the mainstream, the film layer remains attached to the surface as long as the blowing rate does not exceed about 0.5. At higher blowing rates, the mainstream will wrap around and underneath the separated film, reducing its effectiveness. But high film injection velocities cannot always be avoided in turbine cooling applications because of the pressure drop needed across the outer shell of the airfoil to insure that a positive flow direction is always maintained. High blowing rates are a particular problem with multiple rows of film cooling holes fed from a common supply plenum and discharging into a region of rapidly varying freestream static pressure.

To delay separation to much higher blowing rates, film cooling holes can be oriented at a compound angle to the surface and mainstream in local areas on the turbine blade where the boundary layer has a tendency to separate such as in the diffusion region on the suction or convex side of the blade. Where the film-to-mainstream velocity ratio (or in general the ρu ratio) can be kept low however, and the boundary layer is not already near separation, in-line injection is preferred because it causes less turbulent mixing and consequently the film persists longer. Also, in-line injection results in a lower aerodynamic penalty in turbine efficiency because most of the momentum of the film jet is recovered.

REFERENCES

1. Eriksen, V. L., "Film Cooling Effectiveness and Heat Transfer With Injection Through Holes", HTL-TR-102, Aug. 1971, Minnesota Univ., Minneapolis, Minnesota.

2. Liess, C., "Film Cooling with Ejection From a Row of Inclined Circular Holes. An Experimental Study for the Application to Gas Turbine Blades", VKI-TN-97, Mar. 1974, Von Karman Institute For Fluid Mechanics, Rhode-Saint-Genese, Belgium.

3. Choe, H., Kays, W. M., and Moffat, R. J., "The Superposition Approach to Film Cooling", ASME Paper 74-WA/HT-27, New York, N.Y., Nov. 1974.

4. Crawford, M. E., Choe, H., Kays, W. M., and Moffat, R. J., "Full-Coverage Film Cooling Heat Transfer Studies- A Summary of the Data for Normal-Hole Injection and 30° Slant-Hole Injection", HMT-19, 1975, Stanford University, Stanford, Calif.

5. Mayle, R. E , and Camerata, F. J., "Multi-hole Cooling Film Effectiveness and Heat Transfer", ASME Paper No. 74-HT-9, Boston, Mass., July 1974.

6. LeBrocq, P. V., Launder, B. E., and Priddin, C. H., "Discrete Hole Injection as a Means of Transpiration Cooling - An Experimental Study", HTS/71/37, 1971, Imperial College of Science and Technology, London, England.

7. Launder, B. E., and York, J., "Discrete Hole Cooling in the Presence of Freestream Turbulence and a Strong Favorable Pressure Gradient", HTS/73/9, Jan. 1973, Imperial College of Science and Technology, London, England.

8. Hale, R. W., Tan, P., Stowell, R. C., and Ordway, D. E., "Development of an Integrated System for Flow Visualization in Air Using Neutrally-Buoyant Bubbles", SAI-RR-7107, Dec. 1971, Sage Action, Inc., Ithaca, N.Y.

9. Colladay, R. S., Russell, L. M., and Lane, J. M., "Streakline Flow Visualization of Discrete Hole Film Cooling - Holes Inclined 30° to the Surface", NASA Technical Note (to be published).

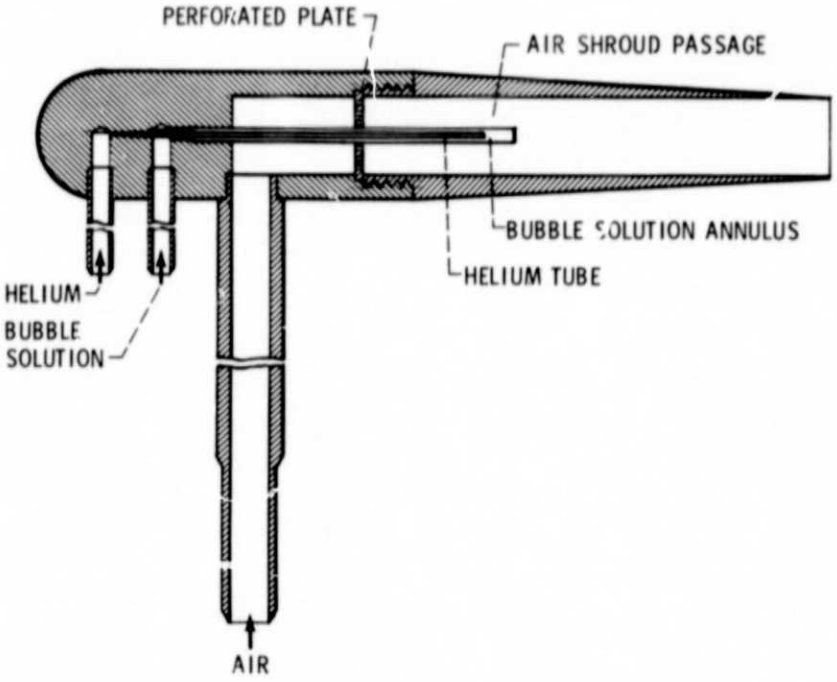

Figure 1. - Bubble generator head.

E-8418

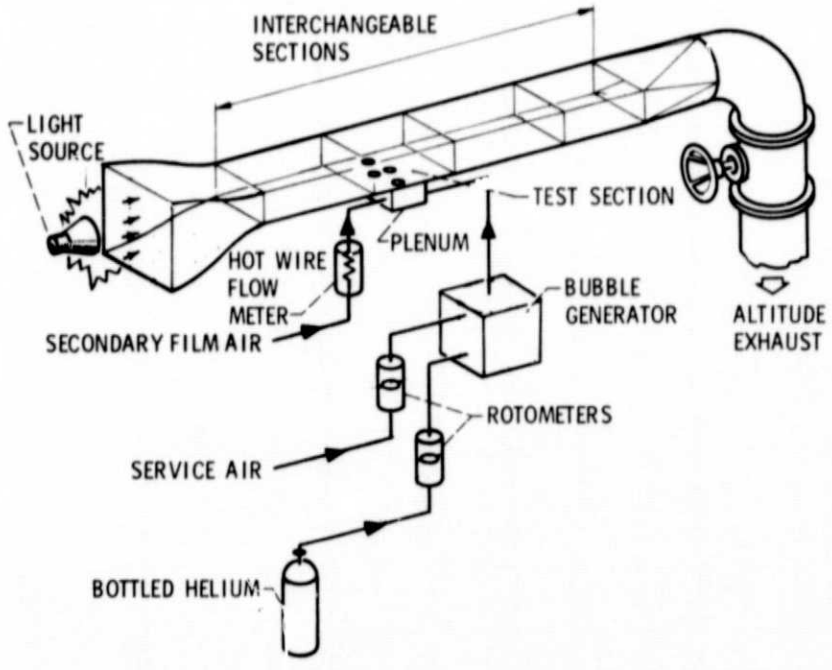

Figure 2. - Film cooling f ow visualization rig.

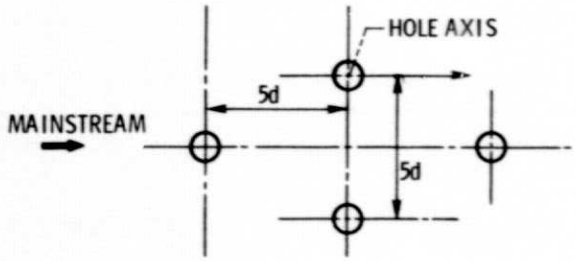

(a) NORMAL.

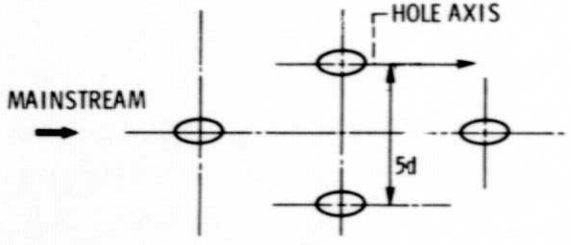

(b) SLANTED 30° IN-LINE.

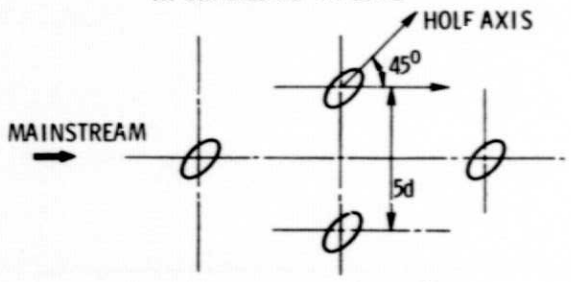

(c) COMPOUND ANGLE 30° BY 45°.

Figure 3. - Top view of the three injection arrays.

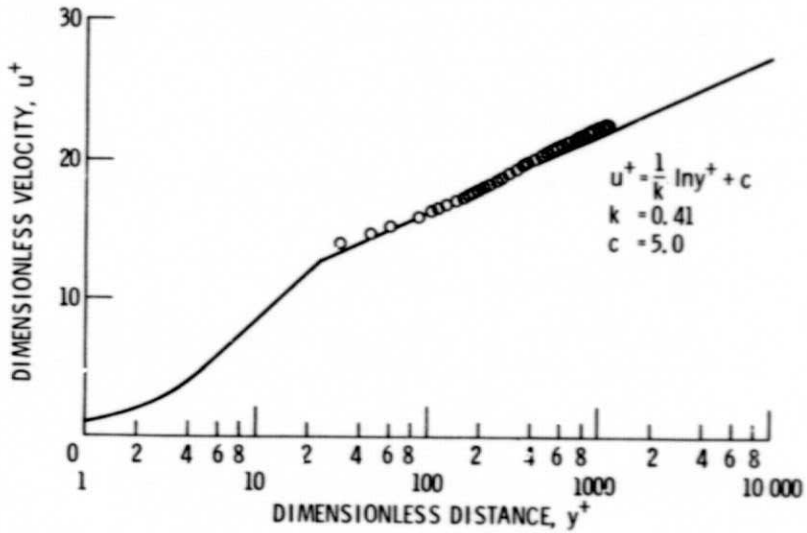

Figure 4. - Boundary layer profile at the upstream injection location.

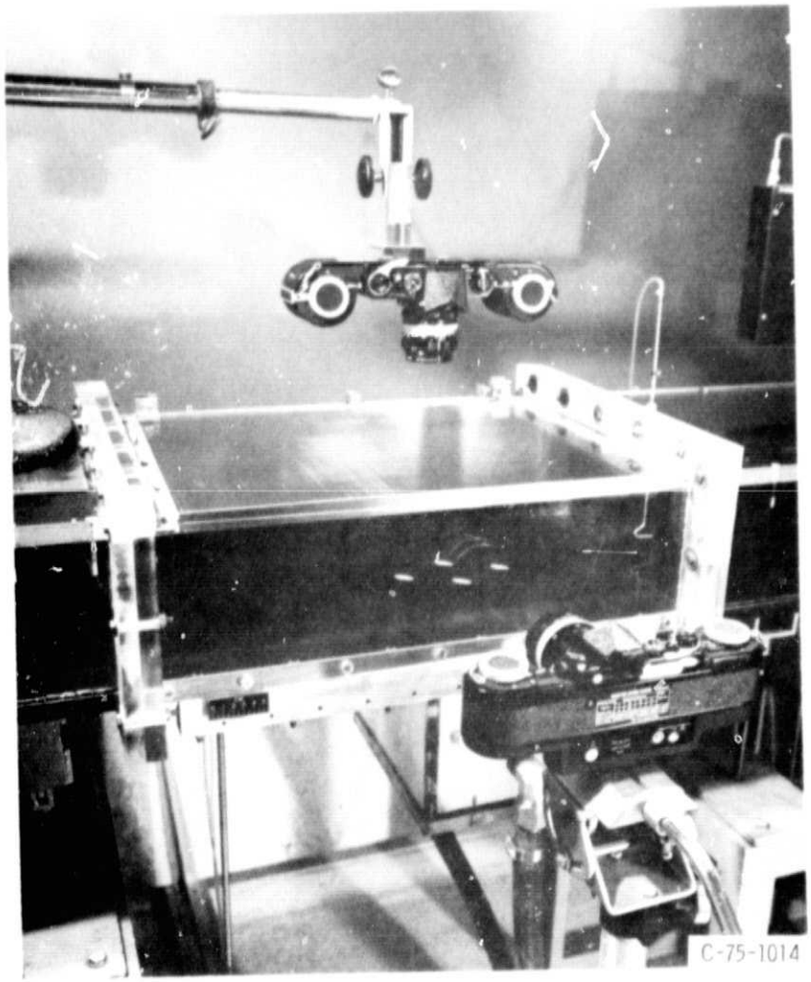

Figure 5. - Test section with top and side view camera positions.

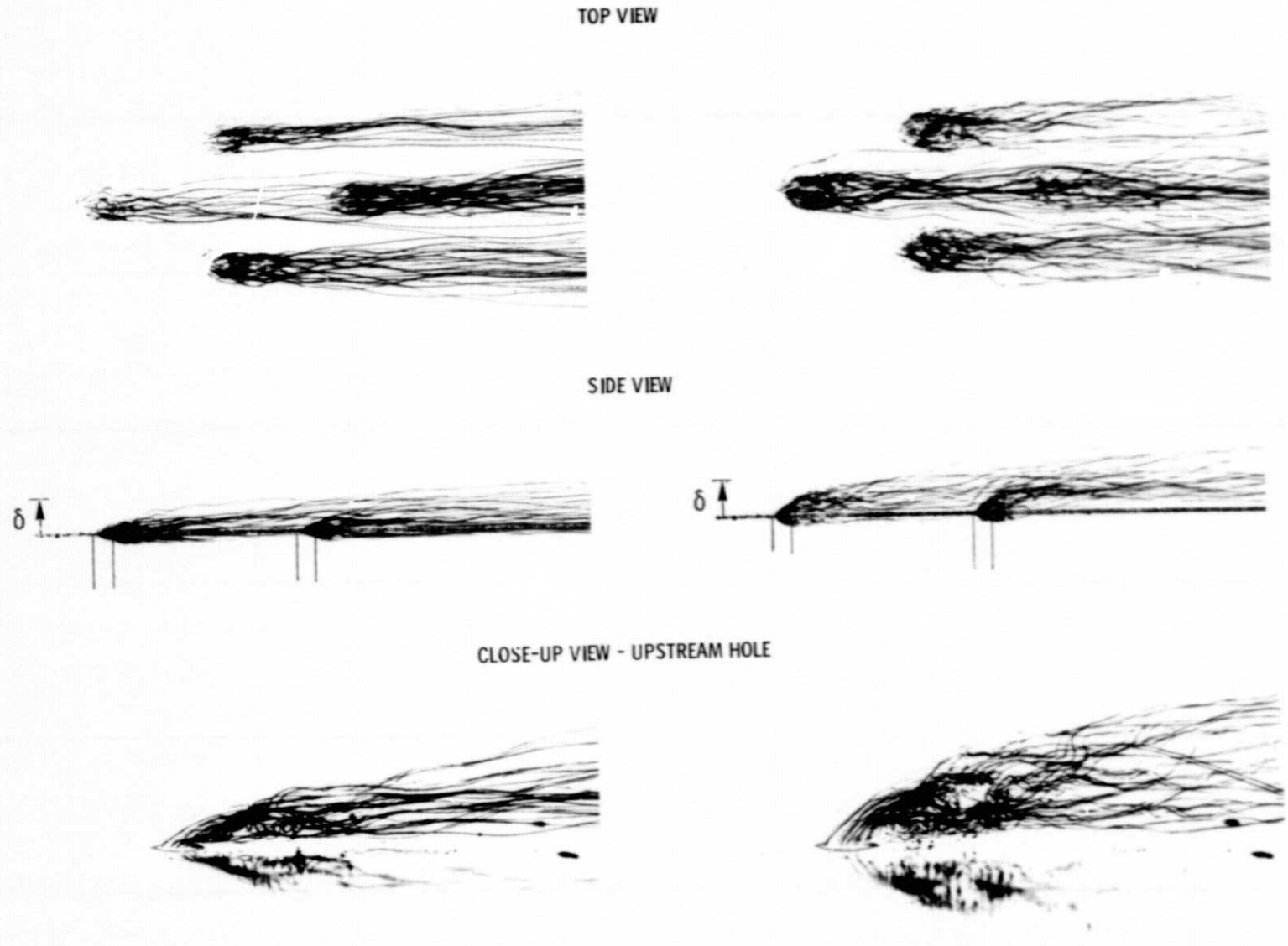

(a) VELOCITY RATIO, m = 0.3.

(b) VELOCITY RATIO, m = 0.8.

Figure 6. - Streakline pattern for film injection from holes normal to the surface.

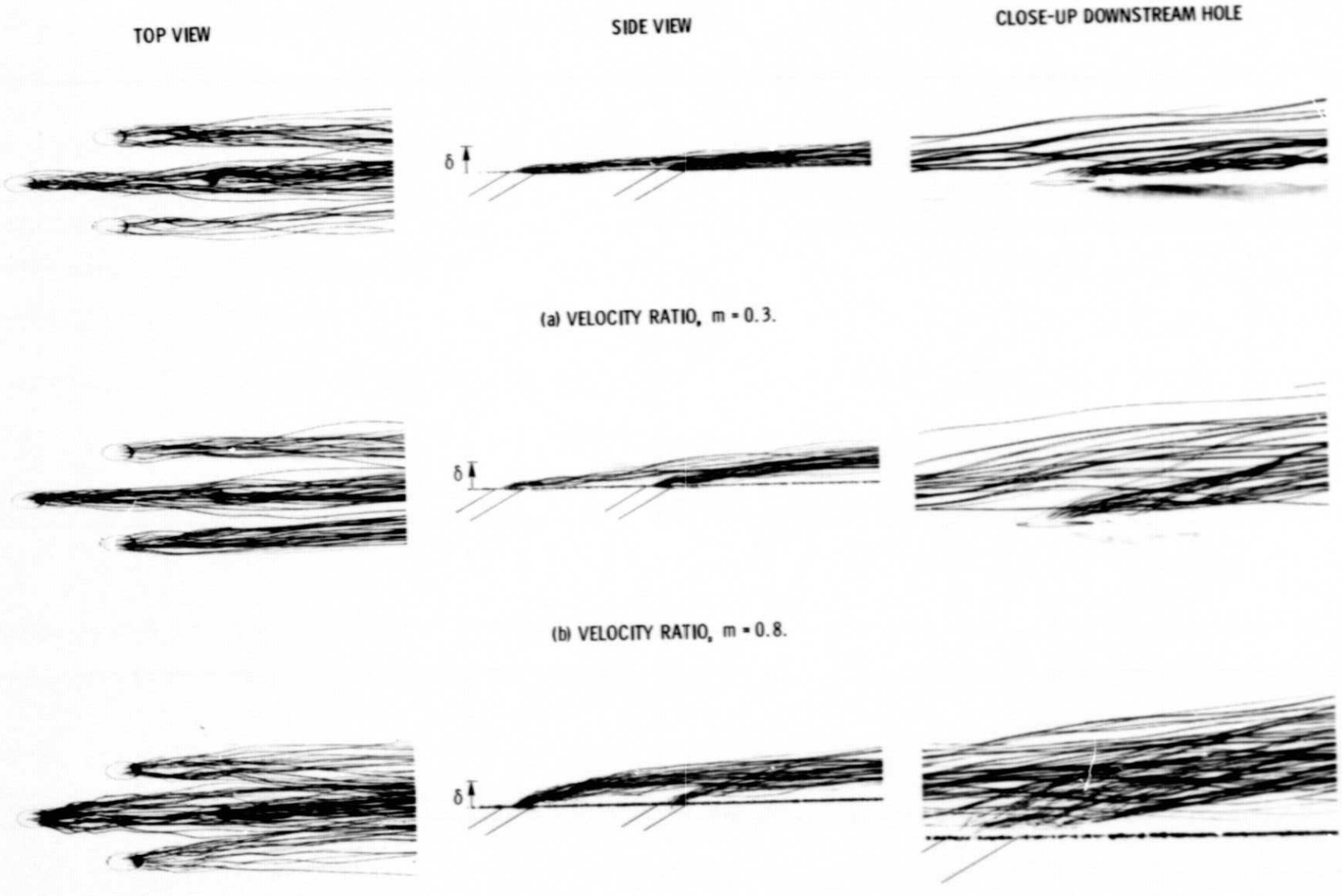

(a) VELOCITY RATIO, m = 0.3.

(b) VELOCITY RATIO, m = 0.8.

(c) VELOCITY RATIO, m = 1.4.

Figure 7. - Streaklines for film injection from holes angled 30^0 to the surface in-line with the mainstream.

(a) VELOCITY RATIO, m = 0.3.

(b) VELOCITY RATIO, m = 0.75.

(c) VELOCITY RATIO, m = 0.75. CLOSE-UP OF UPSTREAM HOLE.

Figure 8. - Compound angle film injection - top view.

(a) VELOCITY RATIO, m = 0.3.

(b) VELOCITY RATIO, m = 0.9.

Figure 9. - Compound angle injection - side view.

Figure 10. - In-line, 30° injection into a thick boundary layer.

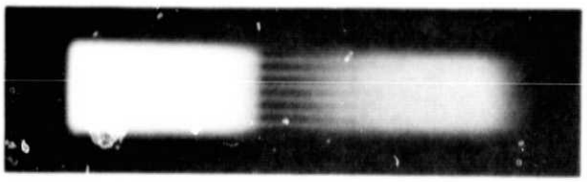

(a) SLANTED IN-LINE INJECTION, 30°.

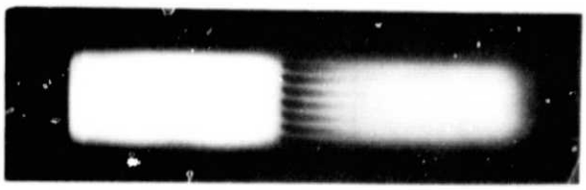

(b) COMPOUND ANGLE INJECTION, 30°x45°.

Figure 11. - Infrared thermal image of a discrete hole film-cooled wall.